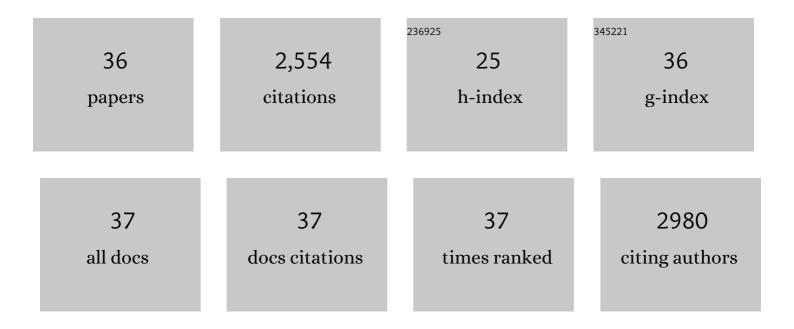
## **Xuelong Wang**

List of Publications by Year in descending order

Source: https://exaly.com/author-pdf/8451119/publications.pdf Version: 2024-02-01



XUELONG WANG

#	Article	IF	CITATIONS
1	General Descriptors for CO <sub>2</sub> -Assisted Selective C–H/C–C Bond Scission in Ethane. Journal of the American Chemical Society, 2022, 144, 4186-4195.	13.7	26
2	Additive engineering for robust interphases to stabilize high-Ni layered structures at ultra-high voltage of 4.8 V. Nature Energy, 2022, 7, 484-494.	39.5	138
3	Reaction-driven selective CO <sub>2</sub> hydrogenation to formic acid on Pd(111). Physical Chemistry Chemical Physics, 2022, 24, 16997-17003.	2.8	5
4	The Role of Electron Localization in Covalency and Electrochemical Properties of Lithiumâ€lon Battery Cathode Materials. Advanced Functional Materials, 2021, 31, 2001633.	14.9	21
5	Identification of LiH and nanocrystalline LiF in the solid–electrolyte interphase of lithium metal anodes. Nature Nanotechnology, 2021, 16, 549-554.	31.5	171
6	Oxygen-redox reactions in LiCoO2 cathode without O–O bonding during charge-discharge. Joule, 2021, 5, 720-736.	24.0	56
7	Cesium-Induced Active Sites for C–C Coupling and Ethanol Synthesis from CO <sub>2</sub> Hydrogenation on Cu/ZnO(0001ì) Surfaces. Journal of the American Chemical Society, 2021, 143, 13103-13112.	13.7	47
8	Rationalization of promoted reverse water gas shift reaction by Pt3Ni alloy: Essential contribution from ensemble effect. Journal of Chemical Physics, 2021, 154, 014702.	3.0	6
9	Anionic redox induced anomalous structural transition in Ni-rich cathodes. Energy and Environmental Science, 2021, 14, 6441-6454.	30.8	33
10	Local structure adaptability through multi cations for oxygen redox accommodation in Li-Rich layered oxides. Energy Storage Materials, 2020, 24, 384-393.	18.0	101
11	Oxysulfide Li2BeSO: A potential new material for solid electrolyte predicted from first principles. Journal of Alloys and Compounds, 2020, 818, 152844.	5.5	1
12	Investigations on the Fundamental Process of Cathode Electrolyte Interphase Formation and Evolution of High-Voltage Cathodes. ACS Applied Materials & Interfaces, 2020, 12, 2319-2326.	8.0	186
13	Pair distribution function analysis: Fundamentals and application to battery materials. Chinese Physics B, 2020, 29, 028802.	1.4	23
14	Size effect on the growth and pulverization behavior of Si nanodomains in SiO anode. Nano Energy, 2020, 78, 105101.	16.0	51
15	Nucleation and Initial Stages of Growth during the Atomic Layer Deposition of Titanium Oxide on Mesoporous Silica. Nano Letters, 2020, 20, 6884-6890.	9.1	23
16	Depth-dependent valence stratification driven by oxygen redox in lithium-rich layered oxide. Nature Communications, 2020, 11, 6342.	12.8	34
17	Mn Ion Dissolution Mechanism for Lithium-Ion Battery with LiMn <sub>2</sub> O <sub>4</sub> Cathode: <i>In Situ</i> Ultraviolet–Visible Spectroscopy and <i>Ab Initio</i> Molecular Dynamics Simulations. Journal of Physical Chemistry Letters, 2020, 11, 3051-3057.	4.6	60
18	Increasing Poly(ethylene oxide) Stability to 4.5 V by Surface Coating of the Cathode. ACS Energy Letters, 2020, 5, 826-832.	17.4	192

XUELONG WANG

#	Article	IF	CITATIONS
19	High air-stability and superior lithium ion conduction of Li3+3P1-Zn S4-O by aliovalent substitution of ZnO for all-solid-state lithium batteries. Energy Storage Materials, 2019, 17, 266-274.	18.0	114
20	Li–Ti Cation Mixing Enhanced Structural and Performance Stability of Liâ€Rich Layered Oxide. Advanced Energy Materials, 2019, 9, 1901530.	19.5	76
21	In-situ visualization of lithium plating in all-solid-state lithium-metal battery. Nano Energy, 2019, 63, 103895.	16.0	109
22	Surface-to-Bulk Redox Coupling through Thermally Driven Li Redistribution in Li- and Mn-Rich Layered Cathode Materials. Journal of the American Chemical Society, 2019, 141, 12079-12086.	13.7	47
23	Unified View of the Local Cation-Ordered State in Inverse Spinel Oxides. Inorganic Chemistry, 2019, 58, 14389-14402.	4.0	21
24	Highâ€Voltage Chargingâ€Induced Strain, Heterogeneity, and Microâ€Cracks in Secondary Particles of a Nickelâ€Rich Layered Cathode Material. Advanced Functional Materials, 2019, 29, 1900247.	14.9	219
25	Anionic Redox Reaction-Induced High-Capacity and Low-Strain Cathode with Suppressed Phase Transition. Joule, 2019, 3, 612.	24.0	3
26	Anionic Redox Reaction-Induced High-Capacity and Low-Strain Cathode with Suppressed Phase Transition. Joule, 2019, 3, 503-517.	24.0	262
27	Another Strategy, Detouring Potential Decay by Fast Completion of Cation Mixing. Advanced Energy Materials, 2018, 8, 1703092.	19.5	30
28	Probing the Complexities of Structural Changes in Layered Oxide Cathode Materials for Li-Ion Batteries during Fast Charge–Discharge Cycling and Heating. Accounts of Chemical Research, 2018, 51, 290-298.	15.6	78
29	Synchrotron Radiation Nanoscale X-ray Imaging Technology And Scientific Big Data Mining Assist Energy Materials Research. Microscopy and Microanalysis, 2018, 24, 542-543.	0.4	0
30	Discovery and design of lithium battery materials via high-throughput modeling. Chinese Physics B, 2018, 27, 128801.	1.4	2
31	Stabilizing Cathode Materials of Lithium-Ion Batteries by Controlling Interstitial Sites on the Surface. CheM, 2018, 4, 1685-1695.	11.7	63
32	Quantitative structure-property relationship study of cathode volume changes in lithium ion batteries using ab-initio and partial least squares analysis. Journal of Materiomics, 2017, 3, 178-183.	5.7	29
33	In situ Visualization of State-of-Charge Heterogeneity within a LiCoO <sub>2</sub> Particle that Evolves upon Cycling at Different Rates. ACS Energy Letters, 2017, 2, 1240-1245.	17.4	159
34	Finding a Needle in the Haystack: Identification of Functionally Important Minority Phases in an Operating Battery. Nano Letters, 2017, 17, 7782-7788.	9.1	42
35	Oxysulfide LiAlSO: A Lithium Superionic Conductor from First Principles. Physical Review Letters, 2017, 118, 195901.	7.8	58
36	Oxygen-driven transition from two-dimensional to three-dimensional transport behaviour in β-Li <sub>3</sub> PS <sub>4</sub> electrolyte. Physical Chemistry Chemical Physics, 2016, 18, 21269-21277.	2.8	66